Phalanx morphology in salamanders: A reflection of microhabitat use, life cycle or evolutionary constraints?

Article *in* Zoology · August 2022

DOI: 10.1016/j.zool.2022.126040

CITATIONS
0

READS
57

3 authors:

Maria Laura Ponssa
National Scientific and Technical Research Council
84 PUBLICATIONS **688** CITATIONS
SEE PROFILE

Jessica Fratani
Unidad Ejecutora Lillo (CONICET - FML) Tucumán - Argentina
18 PUBLICATIONS **84** CITATIONS
SEE PROFILE

Sebastián Barrionuevo
Fundación Miguel Lillo. UEL (Conicet-FML)
32 PUBLICATIONS **554** CITATIONS
SEE PROFILE

Zoology 154 (2022) 126040

Contents lists available at ScienceDirect

Zoology

journal homepage: www.elsevier.com/locate/zool

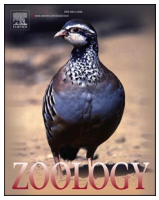

Phalanx morphology in salamanders: A reflection of microhabitat use, life cycle or evolutionary constraints?

María Laura Ponssa [a,*,1], Jessica Fratani [a], J. Sebastián Barrionuevo [a,b]

[a] Área Herpetología, Unidad Ejecutora Lillo (CONICET-Fundación Miguel Lillo), Miguel Lillo 251, S. M. de Tucumán, Argentina
[b] Fundación Miguel Lillo, Miguel Lillo 251, S. M. de Tucumán, Argentina

ARTICLE INFO

Keywords:
Caudata
Finger osteology
Morphological constraints
Microhabitat
Anatomy
Locomotion
Developmental modes

ABSTRACT

Morphological patterns are modeled by the interaction of functional, phylogenetic, ecological, and/or developmental constraints. In addition, the evolution of life cycle complexity can favor phenotypic diversity; however, the correlation between stages of development may constrain the evolution of some organs. Salamanders present microhabitat and life cycle diversity, providing an excellent framework for testing how these factors constrain phenotypic evolution. We reconstructed the morphological evolution of the terminal phalanx using a sample of 60 extinct and living species of salamanders. Using a geometric morphometric approach combined with comparative analyses, we further investigated the impact of phylogenetic, ecological, and/or life cycle factors on the shape of the terminal phalanx. We find that the phylogeny has some influence in determining the dorsal shape of the phalanges; whereas a relationship between microhabitat or life cycle and the dorsal and lateral shapes of the phalanx was not observed in the analyzed species. The allometric pattern found in the phalanx shape implies that small phalanges are more curved and with more truncated end than bigger phalanges. The evolutionary rate of phalanx shape was higher in the semiaquatic species, and the morphological disparity was significantly higher on biphasic groups. These results contradict the hypothesis that a complex life cycle constrains body shape. Finally, the phalanx shape of the salamander remains quite conserved from the Mesozoic. This configuration would allow them to occur in the different microhabitats occupied by the salamander lineages.

1. Introduction

The shape of an organism is a more or less integrated set of traits that can result from phylogenetic, ecological, mechanical, and/or developmental constraints (Blomberg et al., 2003; Losos, 2011; Edgington and Taylor, 2019). To understand how the emergent traits of systems arise from their interaction with other traits, it is important to infer how a trait acquires its observed shape (Arnold, 1983). Amphibians exhibit a diversity of shapes, habitats and developmental modes, offering a good opportunity for testing how these factors foster phenotypic evolution.

Among amphibians, the Caudata clade display a great diversity with a large geographic distribution (755 species – Frost, 2021; 765 species – AmphibiaWeb, 2021), and provides an excellent framework to conduct research from diverse perspectives, such as systematics and phylogenetics, morphology, development, and ecology (Wake, 2009). Salamanders may be terrestrial, aquatic, arboreal, and semiaquatic, and the locomotor challenges imposed by different environments are solved through different movement patterns. In water, they both swim and walk along the bottom (O' Reilly et al., 2000); their swimming is an undulatory movement (Gray, 1968). On land, salamanders can move by undulation (as in water), or can walk, trot, or even jump (O' Reilly et al., 2000). During the walk, at least three feet are in contact with the substrate at all times (O' Reilly et al., 2000).

Some locomotor features have been associated with the occupation of specific habitats, such as caves, epiphytes (moss and liverwort mats and clusters, bromeliads), leaf axils, soil, and streams (Wake and Lynch, 1976; Wake, 1987; Wake and Campbell, 2001). Some examples of characteristic associations include limb elongation and reduced body and tail size in cave-dwelling species of *Eurycea* (Edgington and Taylor, 2019). Reduced limbs and an increase in the number or length of vertebrae are present in burrowing species of Plethodontidae of the genera *Batrachoseps*, *Oedipina* and *Pseudoeurycea* (Wake, 1966;

* Corresponding author.
E-mail address: mlponssa@hotmail.com (M.L. Ponssa).
[1] ORCID: 0000-0002-8750-9680

https://doi.org/10.1016/j.zool.2022.126040
Received 30 July 2021; Received in revised form 11 July 2022; Accepted 1 August 2022
Available online 6 August 2022

Jockusch, 1997). Expansion of the manus, pes, and interdigital webbing has been associated with cave-dwelling habits in species of *Chiropterotriton* (Jaekel and Wake, 2007). Body miniaturization and limb reduction were related to crevice-dwelling habits in species of *Thorius* (Wake, 2009). Body miniaturization combined with specialized digits and prehensile tails was associated with bromeliad-dwelling habits in species of *Chiropterotriton*, *Cryptotriton*, *Nototriton*, and *Dendrotriton* (Wake and Lynch, 1976; Wake, 1987). Undifferentiated pad was associated with leaf-axil dwelling habits in species of *Bolitoglossa* (Jaekel and Wake, 2007). Interdigital webbing coupled with development of hook on terminal phalanges was related to arboreal habits in *Bolitoglossa* (Wake, 2009). Terminal phalanges distally flattened, expanded and recurved with a proximal process for attachment of ligament was an adaptation in climbers *Aneides* (Larson et al., 1981). In fact, some of these associations are used to infer the behavior and paleohabitats of extinct forms of salamanders (e.g. Estes, 1965; Wang and Gao, 2008; Gao and Shubin, 2012).

Life cycle variation has been frequently involved in shaping patterns of amphibian evolution (Shaffer, 1984; Hanken, 1992; Wake and Hanken, 1996; Wiens and Hoverman, 2008; Bonett et al., 2014), and specific phylogenetic tests have been conducted to explore how life cycle complexity influences trait evolution (Bonett and Blair, 2017; Sherratt et al., 2017; Liedtke et al., 2018; Wollenberg et al., 2017; Edgington and Taylor, 2019; Ledbetter and Bonett, 2019; Bonett et al.,2020; Fabre et al., 2020; Bardua et al., 2021). (The different life stages are likely to undergo different selective pressures through ontogeny (e.g. Ebenman, 1992; Duellman and Trueb, 1994; Vučić et al., 2019). Complex life cycles of salamanders offer compelling systems for testing how developmental processes, such as metamorphosis and the associated changes of habitat, can produce morphological diversity (e.g. Ebenman, 1992; Duellman and Trueb, 1994; Bonett et al., 2021). A biphasic life cycle typically involves a change of habitat after metamorphosis, which is coupled with distinct physiological, morphological and functional changes (e.g. Ebenman, 1992; Duellman and Trueb, 1994; Vučić et al., 2019; Fabre et al., 2020). The evolution of a complex life cycle promotes phenotypic discontinuities across ontogeny; however, adaptations for one stage may compromise evolution to the other (Wake and Roth, 1989; Ebenman, 1992; Bonett and Blair, 2017). This compromise can depend on the studied structure. For example, overall head shape evolution is not constrained by metamorphosis (Vučić et al., 2019). Limb and body form, and vertebral column evolution showed accelerated evolutionary rates in paedomorphic, aquatic and direct developer species (Bonett and Blair, 2017). Hind limb length was found to evolve at a higher rate in paedomorphic salamanders (Ledbetter and Bonett, 2019). Cranial shape exhibits the slowest rates of evolution in direct developers, and the highest in paedomorphic species (Fabre et al., 2020).

It has been suggested that some traits exhibiting heterochronic developmental patterns would be linked to environmental factors (Richarson et al., 2009). For example, larvae of pond-dwelling species (e.g. *Ambystoma mexicanum* or *Triturus dobrogicus*) show great acceleration of forelimb development compared to hind limb development (Richarson et al., 2009). Stream-dwellers species (e.g. *Desmognathus quadramaculatus* and *Dicamptodon tenebrosus*) and terrestrial direct developers (e.g. *Desmognathus aeneus*) show a lower degree of forelimb acceleration (Wake and Shubin, 1998; Franssen et al., 2005). In addition, some traits showed an allometric pattern of growth that would have favored the tendency towards arboreality. This is the case of *Bolitoglossa* species with small body size, in which webbing and reduction of phalanges imply a paedomorphic trait (most likely the result of developmental truncation) (Alberch, 1981).

Terminal phalanges in salamanders are characterized by an ample diversity in morphology. The phenotypic spectrum includes large and distally expanded terminal phalanges (even bifurcated distally in some species) to small nubbin-shaped ones, with many transitional forms in between (Wake, 1963; Wake and Brame, 1966, Alberch, 1981; Darda and Wake, 2015). Although the digit in salamanders has been studied from a comparative morphology perspective, the relationship between digit shape and microhabitat or life cycle complexity is almost unexplored (e.g. Larson et al., 1981; Diefenbacher, 2008).

The goal of this study was to reconstruct the shape evolution of the salamander terminal phalanges in order to disentangle the drivers –phylogenetic, ecological, and/or life cycle factors– of morphological evolution. We first investigated whether the digit shape is related to microhabitat use in Caudata. Taking into account the diversity of this group, we hypothesize that the shape of the phalanges will be associated with the locomotor challenges of displacement in arboreal, terrestrial, aquatic, and semiaquatic environments (Adams and Nistri, 2010; Edgington and Taylor, 2019). As an alternative hypothesis, phylogeny may influence digit morphology, resulting in digit shape variability constrained by the phylogenetic relationships. We also investigated whether life cycles influence digit shape diversity. In addition, we calculated the evolutionary rate and disparity of adult digit phenotypes. We work under the hypothesis that maintaining a complex life cycle constrains body shape; therefore, the evolutionary rate of morphological characters should be increased in simple life cycle forms (Bonett and Blair, 2017). Thus, we expect lower evolutionary rates and disparity in complex (biphasic) life cycle species than in lineages with simple, terrestrial (direct-development) or aquatic-only (paedomorphic) life cycles. Finally, we optimized the gathered morphometric data onto the phylogeny to identify evolutionary tendencies within the group and we tested phylogenetic morphological covariation between dorsal and lateral terminal phalanx configurations. If there were covariation, the latter analysis might allow us to predict one configuration when only the other is available. This may be a useful tool, for example, for the interpretation of fossil habits, in which the available material often does not allow us to analyze multiple views of a skeleton.

2. Materials and methods

2.1. Material and data collection

We examined skeletons of specimens from the herpetological collection of the Field Museum of Natural History (FMNH), Chicago, United States. Material from morphological database DigiMorph (digimorph.org) was also reviewed. The scaled 3D images of these digital repositories were transformed into 2D with a screenshot of the dorsal and lateral views of the phalanges. We also considered scaled photos of published osteological descriptions of 8 species of Caudata. We included 91 adult specimens representing the 9 families (following to Frost, 2021) of Caudata (plus 3 *incertae sedis*), 28 genera and 56 extant and 4 fossil salamander species (see Table 1 and Supporting information S1 for a complete list). Cleared and stained specimens and dry skeletons were examined under a Meiji EMZ-5 binocular microscope. Photographs of the third digit of the right hand were taken with a Nikon Coolpix P6000 camera by the same person (M.L.P.). Photographs included dorsal and lateral views (Fig. 1); phalanges were positioned in the same plane and the same distance was used from the camera to the subject. We did not collect data of sex from these specimens, since the skeletal preparations did not have this information; this fact should be considered in the interpretation of our results.

To test for the relationship of digit shapes with microhabitat and life cycle, we recorded these attributes per species using information from Amphibiaweb (accessed 2021), Brandon (1971), Baken and Adams (2019), Blankers et al. (2012), Bonett and Blair (2017), Edgington and Taylor (2019), Evelyn and Sweet (2018), Fabre et al. (2020), Freeman and Bruce (2001), Jia and Gao (2016), Myers et al. (2022), Papenfuss and Wake (1987), Rodríguez Reyes (2009), Rovito et al. (2010), Uribe-Peña et al. (2000) (Supporting information S1). Categorizing the types of microhabitats is a task that hardly escapes from the subjectivity of the observer, and in the supporting information we reference some impressions in categories assigned in the published literature (which may depend on the populations observed, stages of development, etc.).

Table 1
Species included in this study, microhabitats and life cycles. The microhabitat categories include: Aq = aquatic (N = 11); T = terrestrial (N = 32); SAq = semiaquatic (N = 8); A = arboreal (N = 5). The life cycles include: biphasic (bi) (N = 25), direct development (dd) (N = 17), paedomorphic (pd) (N = 6), and facultative biphasic (f-bi) (N = 7). Only species that are obligate paedomorphic in nature were coded as paedomorphic.

Family	Species	Abbreviations	Microhabitats	Life cycle
Ambystomatidae	*Ambystoma altamirani*	*A alt*	T	bi
Ambystomatidae	*Ambystoma annulatum*	*A ann*	T	bi
Ambystomatidae	*Ambystoma gracile*	*A gra*	T	f-bi
Ambystomatidae	*Ambystoma jeffersonianum*	*A jeff*	T	bi
Ambystomatidae	*Ambystoma macrodactylum*	*A mac*	T	bi
Ambystomatidae	*Ambystoma mexicanum*	*A mex*	Aq	pd
Ambystomatidae	*Ambystoma opacum*	*A opa*	T	bi
Ambystomatidae	*Ambystoma texanum*	*A tex*	T	bi
Ambystomatidae	*Ambystoma tigrinum*	*A tig*	T	f-bi
Amphiumidae	*Amphiuma means*	*A mea*	Aq	pd
Cryptobranchidae	*Andrias japonicus*	*A jap*	Aq	pd
Cryptobranchidae	*Chunerpeton tianyiense*	*C tia*	–	–
Hynobiidae	*Batrachuperus yenyuanensis*	*B yen*	Aq	bi
Hynobiidae	*Paradactylodon persicus*	*P per*	Aq	bi
Hynobiidae	*Onychodactylus japonicus*	*O jap*	T	bi
Plethodontidae	*Aneides lugubris*	*A lug*	A	dd
Plethodontidae	*Bolitoglossa helmrichi*	*B hel*	A	dd
Plethodontidae	*Bolitoglossa zacapensis*	*B zac*	A	dd
Plethodontidae	*Chiropterotriton chiropterus*	*C chi*	A	dd
Plethodontidae	*Chiropterotriton magnipes*	*C mag*	T	dd
Plethodontidae	*Desmognathus fuscus*	*D fus*	SAq	bi
Plethodontidae	*Desmognathus monticola*	*D mon*	T	bi
Plethodontidae	*Desmognathus ochrophaeus*	*D och*	T	bi
Plethodontidae	*Desmognathus ocoee*	*D oco*	T	bi
Plethodontidae	*Desmognathus quadramaculatus*	*D qua*	SAq	bi
Plethodontidae	*Desmognathus wrighti*	*D wri*	T	dd
Plethodontidae	*Eurycea bislineata*	*E bis*	T	bi
Plethodontidae	*Eurycea cirrigera*	*E cir*	T	f-bi
Plethodontidae	*Eurycea guttolineata*	*E gut*	T	bi
Plethodontidae	*Eurycea longicauda*	*E lon*	T	bi
Plethodontidae	*Eurycea lucifuga*	*E luc*	T	bi
Plethodontidae	*Eurycea pterophila*	*E pte*	Aq	pd
Plethodontidae	*Eurycea spelaea*	*E spe*	T	bi
Plethodontidae	*Eurycea wilderae*	*E wil*	T	bi
Plethodontidae	*Gyrinophilus porphyriticus*	*G por*	SAq	bi
Plethodontidae	*Karsenia koreana*	*K kor*	T	dd
Plethodontidae	*Plethodon cinereus*	*P cin*	T	dd
Plethodontidae	*Plethodon glutinosus*	*P glu*	T	dd
Plethodontidae	*Plethodon jordani*	*P jor*	T	dd
Plethodontidae	*Pseudoeurycea gadovii*	*P gad*	T	dd
Plethodontidae	*Pseudoeurycea leprosa*	*P lep*	T	dd
Plethodontidae	*Thorius adelos*	*T ade*	A	dd
Plethodontidae	*Thorius longicaudus*	*T lon*	T	dd
Plethodontidae	*Thorius narisovalis*	*T nar*	T	dd
Plethodontidae	*Thorius tlaxiacus*	*T tla*	T	dd
Plethodontidae	*Thorius pinicola*	*T pin*	T	dd
Proteidae	*Necturus maculosus*	*N mac*	Aq	pd
Rhyacotritonidae	*Rhyacotriton olympicus*	*R oly*	SAq	bi
Rhyacotritonidae	*Rhyacotriton variegatus*	*R var*	SAq	bi
Salamandridae	*Cynops ensicauda*	*C ens*	SAq	bi
Salamandridae	*Lissotriton vulgaris*	*L vul*	SAq	f-bi
Salamandridae	*Notophthalmus viridescens*	*N vir*	SAq	f-bi
Salamandridae	*Pachytriton breviceps*	*P bre*	Aq	bi
Salamandridae	*Pleurodeles waltl*	*P wal*	Aq	f-bi
Salamandridae	*Taricha granulosa*	*T gra*	T	f-bi
Sirenidae	*Siren lacertina*	*S lac*	Aq	pd
Sirenidae	*Siren intermedia*	*S int*	Aq	pd
Insertae sedis (hynobiid like)	*Nuominerpeton aquilonaris*	*N aqu*	T	–
Insertae sedis	*Pangerpeton sinensis*	*P sin*	–	–
Insertae sedis	*Beiyanerpeton jianpingensis*	*B jia*	–	–

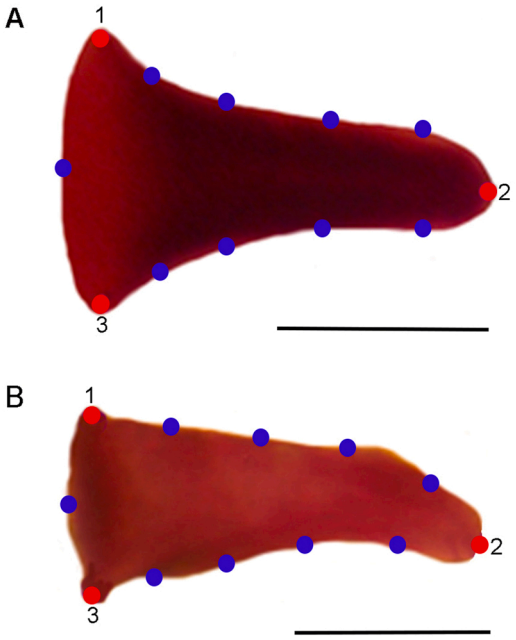

Fig. 1. Landmarks and semilandmarks digitized in the Digit III of the right hand of salamanders. Dorsal view of *Ambystoma tigrinum* (FMNH 53905) (A); lateral view of *Ambystoma macrodactylum* (FMNH 11277) (B). Landmarks and semilandmarks are represented in red and blue, respectively. Scale bar = 1 mm.

Finally, in Table 1 we summarize the categories assigned for our analyzes, according to the material examined and the most precise descriptions of the microhabitat of the species, following microhabitat

categories: arboreal (A), terrestrial (T), aquatic (Aq), and semiaquatic (SAq). The diversity of microhabitats is more complex than the categories defined in the 'microhabitats' column (Table 1); however, unfortunately, a more precise microhabitat categorization would result in a low representation of some categories and in a strongly unbalanced dataset. For this reason, we did not consider cave dwelling as a distinct category in this study. The species previously classified as fossorial or cave dwellers by other authors (Supporting information S1) were considered aquatic or terrestrial according to their main microhabitat. Since images in lateral view were available only for three arboreal species (*Chipterotriton chiropterus*, *Thorius adelos* and *Aneides lugubris*), this microhabitat category must be considered with caution in subsequent results of the lateral view.

2.2. Geometric morphometrics

The dorsal and lateral views of each phalanx were quantified using a combination of three landmarks and nine sliding semilandmarks each (Fig. 1). The two landmark configurations were digitized using StereoMorph 1.6.3 (Olsen and Westneat, 2015). The three landmark datasets included in this study -in dorsal view- correspond to the proximal left angle (LM1), distal tip midpoint (LM2), and the lower right angle (LM3). In lateral view, the landmarks correspond to the lower left angle on the convex side of the digit (LM1), tip midpoint (LM2), and the lower right angle, on the concave side (LM3) (Fig. 1). Landmarks were fixed on homologous points on the phalanges and semilandmarks were allowed to slide along predefined curves while the bending energy was minimized (Bookstein, 1997). One person (M.L.P.) performed all of the digital processing to avoid digitization errors among researchers.

For each configuration (dorsal and lateral), a generalized Procrustes superimposition (Rohlf and Slice, 1990) was performed using geomorph 4.1 (Adams et al., 2021) in R 4.4.1 (R Core Team, 2020). During this procedure, the semilandmarks were permitted to slide along their tangent direction (Guns et al., 2005) in order to minimize Procrustes distance between specimens. From the aligned specimens, a mean shape was calculated for each species. The centroid size of each configuration (dorsal and lateral) was also retained for analysis.

Before conducting the main analyses, a subsample of 20 individuals was digitized twice to account for digitization error, which was not significant (Supporting information S2). We also measured the object asymmetry in the dorsal configuration, which was not significant, and subsequent analyses were performed using the symmetric component (Supporting information S2).

2.3. Phylogenetic framework

Because of shared phylogenetic history, data of species are not independent (Blomberg et al., 2003); therefore, a phylogenetic framework was included for statistical analyses. For that purpose, we built a metatree based on the general topology of Bonett and Blair (2017). We pruned the tree to match our dataset and included those species that were not sampled by Bonett and Blair (2017) using the R library ape 5.5 (Paradis and Schliep, 2019). *Ambystoma altamirani, Batrachuperus persicus, Bolitoglossa zacapensis, Chiropterotriton chiropterus, Thorius adelos, Th. longicaudus, Th. pinicola,* and *Th. tlaxiacus* were included in our metatree following the phylogenetic relationships proposed by Jetz and Pyron (2018), with the same branch lengths as the most closely related lineage. For the phylogenetic projection on the Principal Component Analysis and Ancestral reconstruction of shape (see more details in the following sections), we also included the phylogenetic relationships for the fossil taxa included in our dataset (*Beiyanerpeton jianpingensis, Chunerpeton tianyiense, Nuominerpeton aquilonaris*, and *Pangerpeton sinensis*) based on Rong et al. (2021). In this case, we inferred branch lengths for the whole tree with *compute.brlen* function of library ape 5.5 (Paradis and Schliep, 2019) using Grafen's (1989) method. The metatrees used for our analysis are available in Supporting information S3.

We estimated the degree of phylogenetic signal for both configurations (dorsal and lateral) relative to the Brownian Motion model of evolution using a multivariate K-value, K_{mult} (Adams, 2014). A K-value greater than 1 suggests that there is more phylogenetic signal than expected under Brownian motion, whereas a K-value lower than 1 indicates that a trait is less similar among close relatives and, therefore, has less phylogenetic signal than expected (Blomberg et al., 2003). Statistical significance of all the performed analysis was assessed by permutation (1000 iterations).

2.4. Principal component analysis and phylogenetic generalized least squares

A standard principal component analysis (PCA) with estimated ancestral states and phylogenetic branches projected onto ordination plots was performed to explore patterns of shape variation in dorsal and lateral configurations, including fossils and extant species. We report the principal components (PCs) that explained more than 70 % of shape variation. The phylogeny was projected onto the morphospaces by calculating ancestral states of the internal nodes through maximum likelihood, as implemented in geomorph (Adams et al., 2021). Thin-plate splines warp grids of the PC loadings were used to visualize shape variation described by each PC axis of the phalanges in the morphospaces.

2.5. Phylogenetic Generalized Linear Models (PGLS)

We investigated the impact of allometry in both datasets (dorsal and lateral configurations) using multivariate regressions including phylogeny, in which centroid size calculated from the landmark configurations were used as size parameter. In order to understand the impact of microhabitat and life cycle on shape, we used a Procrustes multivariate analysis of variance (MANOVA) including a phylogenetic framework and using size as a covariate. Fossil taxa were not included in the former analysis due to the lack of ecological information. These analyzes were performed using geomorph 4.4.1 R library (Adams et al., 2021).

2.6. Evolutionary rates

Evolutionary rates were calculated for the dorsal and lateral phalanx shape and compared across different microhabitat and life cycle strategies groups based on a Brownian motion model of evolution using the function *compare.evol.rates* in the geomorph R package 4.4.1 (Adams et al., 2021). For evolutionary rate, the inclusion of groups with four or fewer species should be taken with caution because of possible problems of morphological evolution rate estimation (Adams et al., 2009). In this sense, our results on evolutionary rates of the lateral configuration should be interpreted taking into account that our dataset includes three arboreal species (*Aneides lugubris, Chiropterotriton chiropterus,* and *Thorius adelos*).

2.7. Disparity differences

To assess and compare morphological disparities for each microhabitat (aquatic, semiaquatic, terrestrial, arboreal) and group life cycle strategy (biphasic, paedomorphic, facultative biphasic and direct-development), we used the function *morphol.disparity* in geomorph 4.4.1 (Adams et al., 2021). Disparity was calculated as the Procrustes variance divided by the number of landmarks per bone for each life cycle and microhabitat group using the residuals of a linear model fit containing phylogeny. Differences among groups were identified using pairwise comparisons.

2.8. Phylogenetic reconstruction

To explore the shifts of dorsal and lateral phalanx shape and size

along the phylogeny, we used optimization methods to reconstruct ancestral states via maximum parsimony algorithms in TNT 1.5 (Catalano et al., 2010; Goloboff et al., 2003, 2008; Goloboff and Catalano, 2011, 2016). By default, TNT considers each configuration as roughly equivalent to that of a discrete character (Catalano et al., 2010). The shape reconstruction of ancestral states was performed without implied weights, combining grids and observed state optimization, with six by six grid cells. Since TNT permits the use of missing characters, all the sampled taxa and were included in the optimization.

2.9. Phylogenetic integration

To quantify the degree of phylogenetic morphological covariation between dorsal and lateral phalanx configurations, we performed a partial least squares analysis under a Brownian motion model of evolution using function *integration.test* from geomorph (Adams and Felice, 2014; Adams and Collyer, 2016).

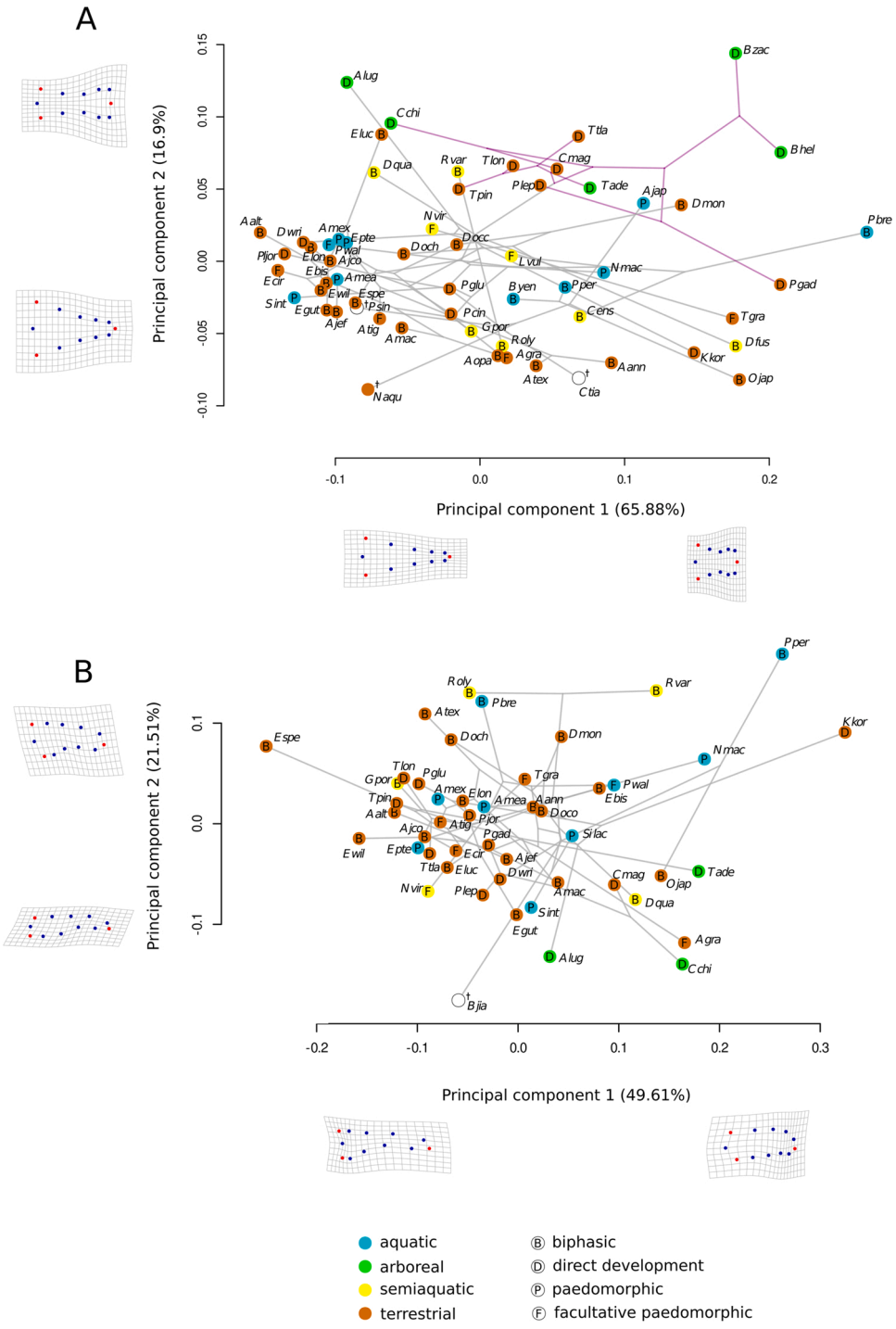

Fig. 2. Phylomorphospace of the (A) anterior phalanx configuration. The clade composed of *Thorius*, *Chiropterotriton*, *Pseudoeurycea* and *Bolitoglossa* species is highlighted in purple. (B) lateral phalanx configuration. Species are colored according to their microhabitat. Deformation grids depict the mean shape of the maximal and minimum score for each principal component.

3. Results

3.1. Dorsal configuration

The PCA showed a great contribution of the first two PCs (Fig. 2A, Supporting information S4). PC1, which accounted for 65.88 % of the total variance, represented shape changes from a narrower to a broader distal end of the terminal phalanges. PC2 accounted for 16.9 % of the total variance. Besides reflecting some of the shape change in the distal end of the phalanges, PC2 also described the variation from a broader to a narrower proximal end. There is a general overlap among species of different ecological categories. The projection of the phylogeny shows that closely related species substantially diverge in the morphospace. The clade formed by *Thorius*, *Chiropterotriton*, *Pseudoeurycea* and *Bolitoglossa* species tends to occupy the region of maximum variation of both PCs (Fig. 2A). Other clades show no pattern in the phylomorphospace, with a general crisscrossed distribution of terminal taxa, indicating that species with different microhabitats and life cycles secondarily evolved similar dorsal configuration of phalanges. Nevertheless, dorsal landmark configuration showed a relatively low but significant phylogenetic signal (K = 0.26; $P = 0.02$; Z = 1.8985).

Phylogenetic MANOVA indicated no significant evidence of an effect of microhabitat (Z = 0.8001; $P = 0.22$) or life cycle (Z = 1.0954; = 0.85) on phalanx shape. A significant evolutionary allometric effect ($R^2 = 17.5$; $P < 0.01$; Z = 2.9856) showed a shift from an 'hourglass shape' to a more 'rhomboid' phalanx shape (Fig. 3). This general tendency had a homogeneous pattern among the different analyzed factors (microhabitat and life cycle).

There was no difference in the evolutionary rates of the dorsal shape evolution for microhabitat ($P = 0.76$; Z = − 0.7719) or life cycle groups ($P = 0.14$; Z = 1.0337) (Fig. 4). The morphological disparity was not significantly different for microhabitat, with similar values among categories (Fig. 5A). Regarding life cycles, biphasic taxa showed significantly higher morphological disparity than facultative biphasic ($P < 0.01$; absolute difference = 0.098) and paedomorphic species ($P = 0.038$; absolute difference = 0.129), and no difference when compared to direct developing species ($P = 0.466$; absolute difference = 0.058) (Fig. 5B).

3.2. Lateral configuration

The PCA of the lateral configuration also showed a great contribution of the first two PCs (Fig. 2B, Supporting information S4). The PC1, which accounted for 49.61 % of the total variance, represented shape changes from a sharper to a blunter distal end of the phalanges. PC1 showed a gradual shift from a concave to a more convex shape of the proximal end, from a concave to a flatter ventral surface, and from a more dorsoventrally compressed to a tall shape of the phalanges. PC2 accounted for 21.51 % of the variance and reflected a shift from a flat to a tall shape. A general overlap was observed among species of different microhabitat, life cycle categories, and clades on the phylomorphospace. In lateral configuration, closely related species tended to diverge greatly in shape, a pattern also shown in dorsal configuration. Lateral landmark configuration showed a low and non-significant phylogenetic signal (K = 0.067; $P = 0.89$; Z = − 1.3887).

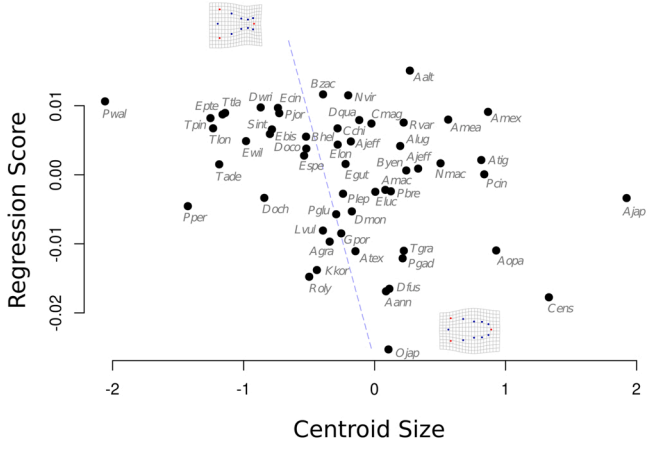

Fig. 3. Allometry plot for dorsal phalanx configuration. A prediction slope is represented by a dotted line. Deformation grids depict the mean shape of the maximal and minimum predicted shapes, and are magnified by a factor of three to facilitate visual interpretation. See Table 1 for name references.

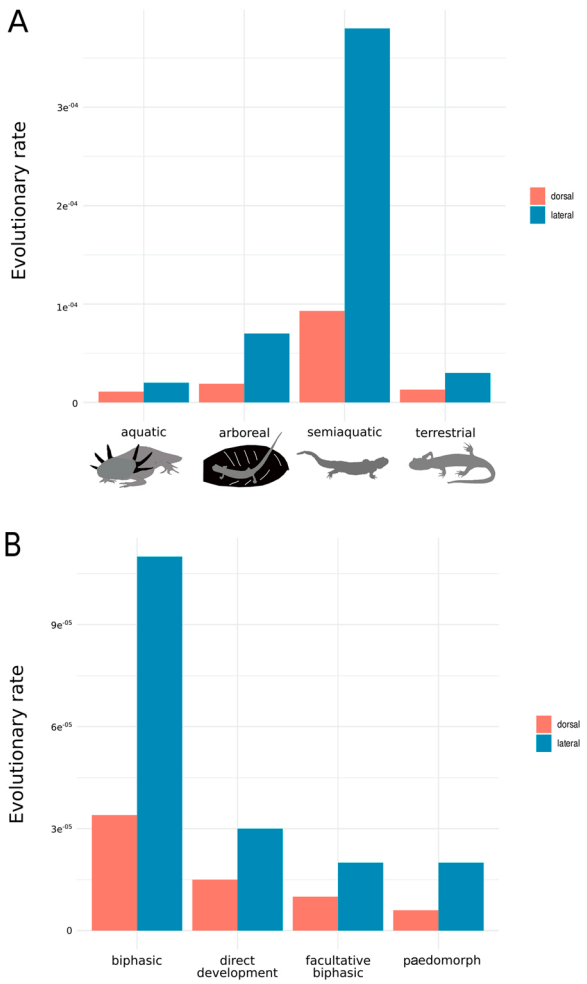

Fig. 4. Histogram of phalanx rate of shape evolution for the different groups by (A) microhabitats and (B) life cycles.

Phylogenetic MANOVA results showed no significant impact of microhabitat (Z = 0.8896; $P = 0.2$) or life cycle (Z = − 1.1605; $P = 0.866$) on lateral phalanx shape. A significant evolutionary allometric effect ($R^2 = 58.49$; $P < 0.01$; Z = 2.6007) was observed, showing a tendency of bigger species to have a slightly blunter phalanx (Fig. 6). As in the dorsal configuration, this general tendency in lateral view was also a homogeneous pattern between the different analyzed factors (microhabitat and life cycle).

There was a significant difference in the evolutionary rates of lateral shape evolution for species microhabitat ($P = 0.02$; Z = 1.7651), but not for life cycle groups ($P = 0.61$; Z = − 0.1782). Semiaquatic taxa showed a higher evolutionary rate than the species with other types of microhabitats (Fig. 4A). Morphological disparity was not significantly different among microhabitat or life cycle categories (Fig. 5).

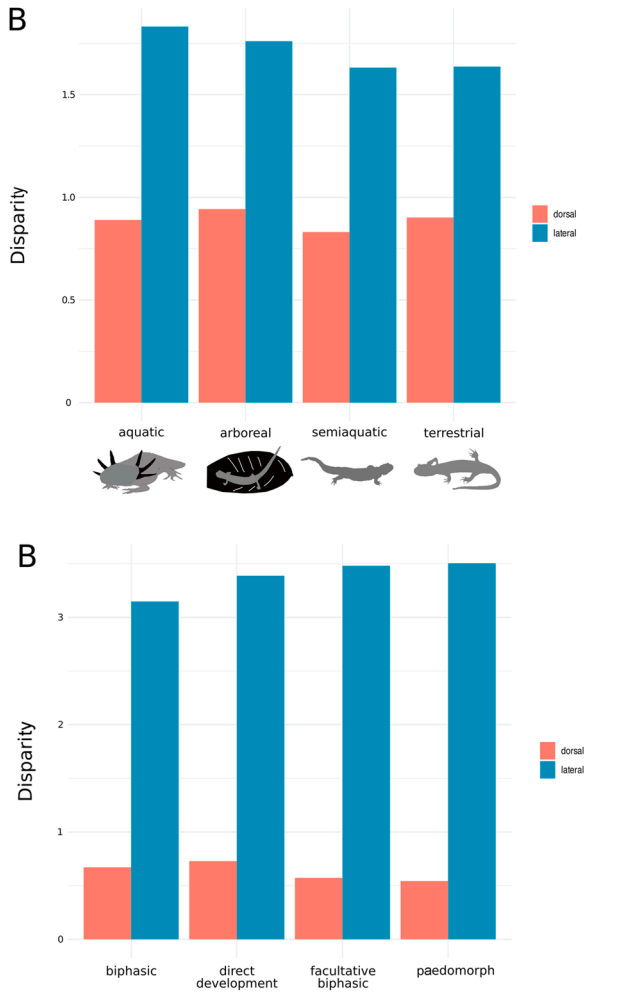

Fig. 5. Histogram of phalanx phenotypic disparity for the different groups by (A) microhabitats and (B) life cycles.

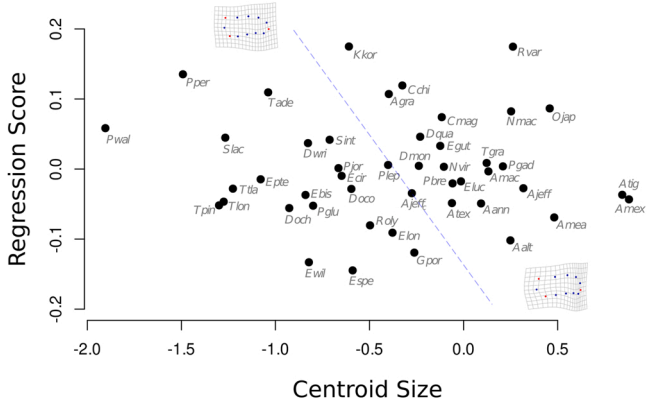

Fig. 6. Allometry plot for lateral phalanx configuration. A prediction slope is represented by a dotted line. Deformation grids depict the mean shape of the maximal and minimum predicted shapes, and are magnified by a factor of three to facilitate visual interpretation. See Table 1 for name references.

3.3. Ancestral shape estimation (Fig. 7)

Optimization of phalanx centroid size on the phylogenetic hypothesis revealed an estimated ancestral average size, with independent cases of increase (*Andrias japonicus, Amphiuma means, Cynops ensicauda, Plethodon cinereus, Ambystoma opacum*, and the clade *A. tigrinum* + *A. mexicanum*) and decrease in size (*Pleurodeles waltl*, *Paradactylodon persicus*, *Thorius* clade and *Eurycea pterophila*) (Fig. 7).

The reconstruction of the dorsal shape indicated generalized triangular ancestral shapes. A shift to a slightly narrower distal end was recorded in the ancestor of *Ambystoma* and *Eurycea*. Within Salamandridae, the ancestral shape of the clade composed of all sister clades of *Pleurodeles waltl* also showed a narrower distal end, but with a truncated tip. A shift to a broader distal end was evident in the ancestor of the clade *Thorius* + *Chiropterotriton* + *Pseudoeurycea* + *Bolitoglossa*, and was accentuated in *Bolitoglossa* species. A broader distal end of the phalanx was also independently acquired in the aquatic species *Andrias japonicus* and *Pachytriton breviceps*, in the terrestrial species *Desmognathus monticola* and *Thorius tlaxiacus*, and in the arboreal *Aneides lugubris*.

Reconstruction of lateral shape showed a mildly curved pattern as the predominant ancestral shape, with changes occurring mostly at the species level. A shift to a slightly narrower phalanx was detected in the ancestors of *Eurycea* and *Rhyacotriton*.

3.4. Relationship between dorsal and lateral configurations

The phylogenetic morphological covariation between dorsal and lateral configurations was significant (r-PLS = 0.584; $P < 0.01$; Z = 2.7714; Fig. 8). Phalanges with a narrower distal end in dorsal view correlated with a sharper and curved shape in lateral view, whereas phalanges with a broader distal end in dorsal view also showed a blunter distal end shape in lateral view.

4. Discussion

A major goal in evolutionary biology is to explain the morphological diversity of species, which often arises from many different mechanisms, including environmental influences, structural or functional constraints, or shared evolutionary history (Wainwright and Reilly, 1994; Gould, 2002; Blomberg et al., 2003; Losos, 2011). Our results show evidence that phylogeny has a significant -although low- effect in the dorsal shape of the phalanges in salamanders, whereas the other factors analyzed (habitat and life cycle) have no significant effect. We also found that phalanx shape responds to an allometric effect. The evolutionary rate differed according to microhabitat groups in the lateral shape, being higher in the semiaquatic species; and the disparity was significantly different only in the dorsal shape of the groups with different life cycle. Ancestral phalanx in salamanders would present an intermediate size and a fairly conserved triangle-like shape in dorsal view. The shape evolved to a distally expanded shape, which is particularly evident in the arboreal *Aneides lugubris* and *Bolitoglossa*, dorsally; and to a slenderer phalanx in some species of the clade *Eurycea* and *Rhyacotriton*, laterally.

The dorsal shape of the terminal phalanges in salamanders is partly explained by common ancestry, since the phylogenetic signal was significant but low (according to the Brownian Motion model). The phylogenetic structure in shape could be driven by the clade formed by *Thorius*, *Chiropterotriton*, *Pseudoeurycea* and *Bolitoglossa* which occupies a particular region of the morphospace defined by a broader distal end of terminal phalanges (Fig. 2A). During locomotion, digits play a primary mechanical role, since they resist the compression force given by a large part of the body weight that acts upon them (Abdala et al., 2022). In tetrapods (except amphibians), the phalanx phenotype has been associated with different habitat uses (Russell and Bauer, 1989; Tulli et al., 2009; Maiolino et al., 2011). Our results do not reveal that the mechanical characteristics of the microhabitats where salamanders move impose restrictions on the shape variability of the terminal phalanx. This can be due to possible uncertainties in assigning species to microhabitats, or it could be microhabitat features that are not represented in our coding. For example, we do not consider categories as saxicolous and fossorial. Similarly, Blankers et al. (2012) and Baken and Adams (2019) found no significant relationship between variation in external characters and microhabitat in plethodontid salamanders. Actually,

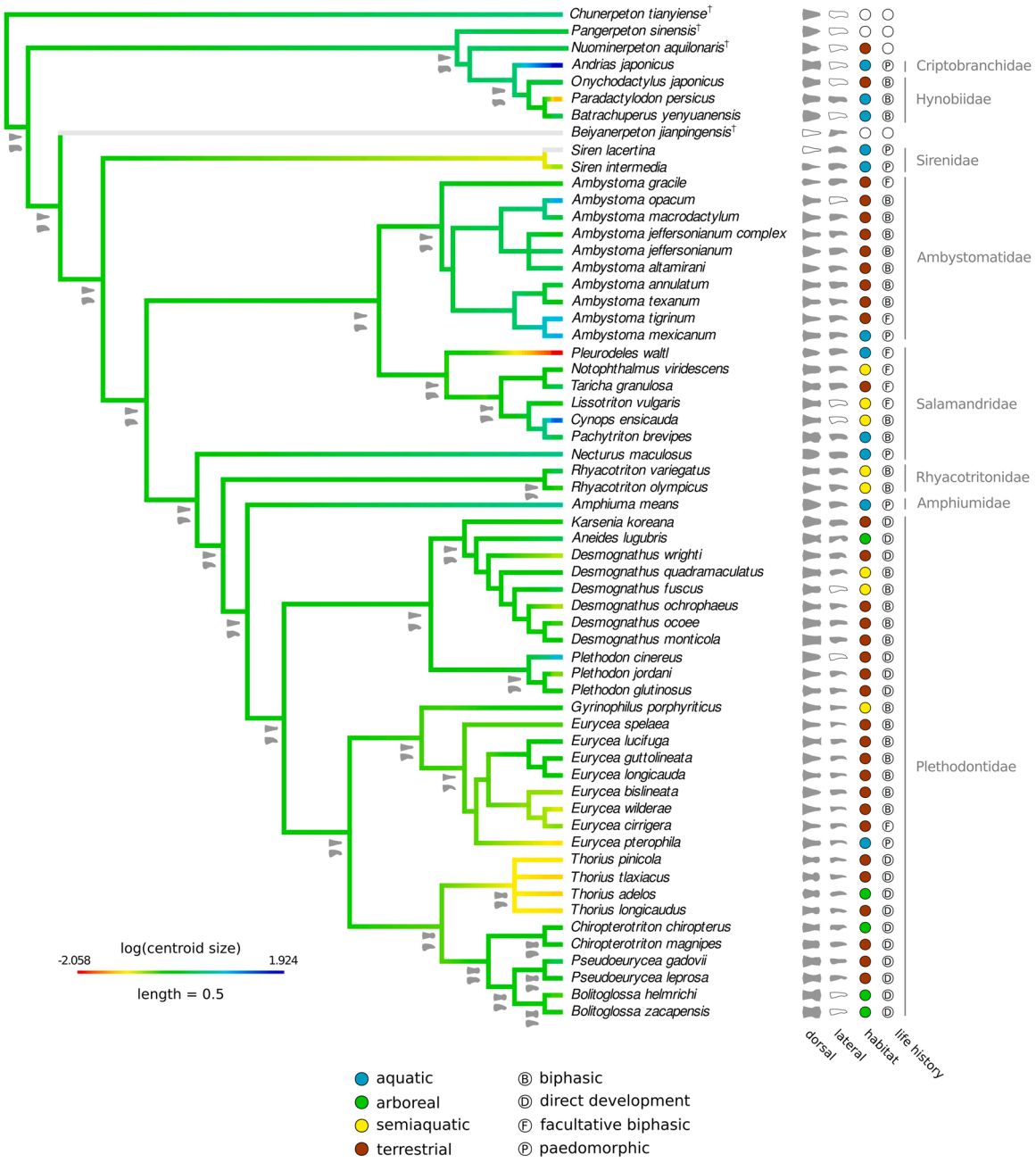

Fig. 7. Ancestral reconstruction of phalanx shape in dorsal and lateral views. The tree branches are colored according to the optimization of the centroid size of the dorsal configuration. Centroid size is represented by the chromatic scale (warm to cold colors representing from small to big sizes) (see scale bar). Microhabitat and life cycle are optimized with a color scheme and letters, respectively (see legend). Empty drawings and gray branches indicate non-available data.

specialization for arboreality would appear only within the relatively recent tropical clade *Bolitoglossa* (Green and Alberch, 1981; Blankers et al., 2012). Blankers et al. (2012) proposed that the strong relationships between morphology and microhabitat use in other tetrapods are not replicated in salamanders because of major differences in behavior and/or physiology between these and salamanders. For example, lizards escape from predators by running speedily (Irschick and Jayne, 1998; Irschick and Losos, 1998; Irschick, 2002). In contrast, the plethodontid salamanders, which have low metabolic rates relative to other amphibians and reptiles (Vitt and Caldwel, 2009), remain immobile as a strategy against predators (e.g. Dodd, 1990). This can advise that the salamanders may be more uniform in their locomotor performance in different microhabitats (Blankers et al., 2012). Alternatively, salamanders may differ significantly in their performance in different microhabitats due to differences in behavior and physiology, but without corresponding variation in morphology (Blankers et al., 2012).

Both dorsal and lateral configuration of the digits of the salamanders would be explained by an evolutionary allometric pattern, which consists of small phalanges more curved and with more truncated end than bigger phalanges. Changes in the pattern of allometric growth between foot surface and body weight -the lighter species show greater adhesiveness- were postulated as an adaptation to optimize the arboreal habits in *Bolitoglossa* species (Alberch, 1981). In the small-sized species of *Bolitoglossa*, webbing would be acquired by developmental truncation, and their small size would be in these cases the main adaptation to arboreality (Green and Alberch, 1981). We can infer the same relationship proposed by the cited authors, since the included arboreal species of *Bolitoglossa* are of moderate to small size (*Bolitoglossa*

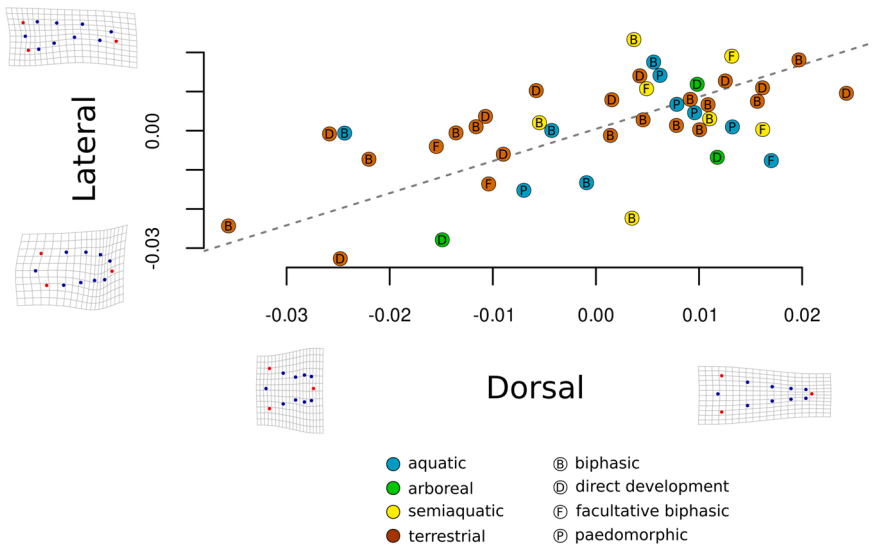

Fig. 8. Phylogenetic morphological covariation plot between the dorsal and lateral phalanx configurations. Species are colored according to their microhabitat and life cycle. Deformation grids depict the predicted shape of the maximal and minimum partial least squares (PLS) score for each component.

zacapensis: mean SVL 4.21 cm in males, and 4.57 cm in females; Parra-Olea et al., 2004; *Bolitoglossa helmrichi*, SVL mean 4.7 cm in males, and 5.6 cm in females; amphibiaweb2021.org), and show the moderate distal expansion described in the smallest arboreal species (Alberch, 1981). This allometric relationship as an adaptation to arboreal living has been proposed at an intrageneric level. In an intergeneric phylogenetic level, this hypothesis would not be supported, since the closest relative of *Bolitoglossa*, the terrestrial *Pseudoeurycea* which has unexpanded fingertips, shows a similar size to that of the *Bolitoglossa* species studied herein (*Pseudoeurycea gadovii*, SVL: 6.3 cm -amphibiaweb2021.org; *Pseudoeurycea helmrichi*, SVL: 5.43 ± 0.65 cm; Gűizado-Rodriguez and García-Vázquez, 2010). Unlike in *Bolitoglossa*, in the *Thorius* clade there is no evidence of an allometric pattern. The distal expansion is similar in terrestrial and arboreal species of the minute *Thorius* (Hanken, 1982; Hanken and Wake, 1994; this study), which are all minute in size (Hanken, 1984; this study). It would be interesting to investigate the factors that have driven invasion of the arboreal habitat in some species of this genus.

The evolution of life cycle simplification stimulates phenotypic diversity (Bonett and Blair, 2017). A complex life cycle, like the biphasic one, would produce phenotypic discontinuities across ontogeny; however, at the same time, specific adaptations for one stage might condition the evolution of a trait to another stage (Hanken, 1992; Moran, 1994; Bonett and Blair, 2017). We found no evidence that life cycle significantly influences phalanx shape rate evolution. Regarding the microhabitat influences on the evolutionary rate, the highest rate values of lateral digit shape evolution in the semiaquatic group associated with a low disparity could be explained by a major morphological change occurring early in the taxa history, leading to very similar morphologies for the group (Michaud et al., 2018). In other morphological characters linked to locomotion, the differences in evolutionary rates would be influenced by microhabitat or the life cycle. For example, Bonett and Blair (2017) showed that body shape and vertebral column evolve faster in species with simpler life cycles (i.e. paedomorphic, aquatic species and direct developers, terrestrial species). Ledbetter and Bonett (2019) found accelerated rates of limb evolution in aquatic species (mostly paedomorphic) in comparison with terrestrial species (mostly direct developers). All these results confirm that the constraints are trait-dependent (Bonett and Blair, 2017; Fabre et al., 2020).

Regarding the disparity of shape, in dorsal view, biphasic life cycle differed significantly from facultative biphasic and paedomorphic life cycles, with disparity being greater in the biphasic species. The digits appear in the aquatic stage in the biphasic species (Fröbisch and Shubin, 2011), but the larval stages might not be a constraint to the morphological diversification of the digits in the terrestrial postmetamorphic stages. An interesting question to be addressed is whether or not the distal phalanges undergo substantial remodeling after metamorphosis; but so far we have no information on this subject.

The phylogenetic covariation between dorsal and lateral configurations allows us to infer, although speculatively, the lateral shape of the distal phalanx of the fossil *Chunerpeton tianyiensis, Pangerpeton sinensis*, and the hynobiid-like *Nuominerpeton aquilonaris*. These extinct species show a narrow distal end, which is correlated with a sharper and curved lateral shape. This correlation would support the interpretation that *Nuominerpeton* was not arboreal – Jia and Gao (2016) infer a near-pond-mountain-brook environment for this salamander–, since, unlike the arboreal *Bolitoglossa, Chiropterotriton chiropterus, Thorius adelos* or *Aneides lugubris*, it does not present an expanded fingertip.

If the ancestor of the salamander had a biphasic life cycle (Bonett and Blair, 2017; Fabre et al., 2020), then, it would have required a functional morphology for effective locomotion in aquatic and terrestrial environments (Bonett and Blair, 2017). Our estimation of ancestral state and the three fossil species (*Nuominerpeton aquilonaris* from Lower Cretaceous, *Chunerpeton tianyiense* and *Pangerpeton sinensis* from Jurassic) shows that ancestral salamanders had digit shape (dorsal shape with a wide base and sharp extreme) and size comparable to that of most of the modern biphasic species (except for *Cynops ensicauda* and *Ambystoma opacum*, which evolved to a larger size). These data suggest that, since then, adult shape in biphasic species would have remained similar. The same pattern was observed in the length and the number of vertebrae (Bonett and Blair, 2017). Both general branch overlap and ancestral shape reconstruction indicate a high level of homoplasy in phalanx shape.

5. Conclusion

Our study adds new evidence to the idea that the constraints of complex life cycles on the evolution of morphology can depend on the studied traits. According to our analyzes, neither the microhabitat nor the life cycle show a relationship with the morphological variability of terminal phalanges in the studied species. The phylogenetic signal in the dorsal shape of the phalanx was significant but low (according to the Brownian Motion model used here). Our prediction that maintaining a complex life cycle constrains body shape does not hold, as shape

disparity was significantly higher in biphasic species. Throughout phylogeny, the morphology of the salamander fingers remains fairly conserved from the Mesozoic ancestors of modern salamanders. This conserved morphology would be optimal enough for the salamander lineage to occupy different habitats.

Declaration of Competing Interest

The authors declare that they have no known competing financial interests or personal relationships that could have appeared to influence the work reported in this paper.

Data Availability

Data will be made available on request.

Acknowledgements

M.L.P is very grateful to Alan Resetar and Joshua Mata for their hospitality in the herpetology collection of the FMNH. We thank to the reviewers and editor for their detailed suggestions and corrections. This work was supported by Agencia Nacional de Promoción Científica y Tecnológica: PICT 2016-2772, 2018-00832, 2019-0346 and 2019-3520; Consejo Nacional de Investigaciones Científicas y Técnicas: PIP 0045, 2108; Field Museum of Natural History; FAPESP Proc. 2013/50741-7.

Appendix A. Supporting information

Supplementary data associated with this article can be found in the online version at doi:10.1016/j.zool.2022.126040.

References

Abdala, V., Ponssa, M.L., Fratani, J., Manzano, A., 2022. The role of hand, feet, and digits during landing in anurans. Zool. Anz. 296, 187–197.
Adams, D.C., 2014. A generalized K statistic for estimating phylogenetic signal from shape and other high-dimensional multivariate data. Syst. Biol. 63, 685–697.
Adams, D.C., Collyer, M.L.,
2016. On the comparison of the strengthof morphological integration acrossmorphometric datasets. Evolution 70 (11), 2623–2631.
Adams, D.C., Nistri, A., 2010. Ontogenetic convergence and evolution of foot morphology in European cave salamanders (Family: Plethodontidae). BMC Evol. Biol. 10, 216.
Adams, D.C., Felice, R., 2014. Assessing phylogenetic morphological integration and trait covariation in morphometric data using evolutionary covariance matrices. PLoS One 9, e94335.
Adams, D.C., Berns, C.M., Kozak, K.H., Wiens, J.J., 2009. Are rates of species diversification correlated with rates of morphological evolution? Proc. R. Soc. B Biol. Sci. 276 (1668), 2729–2738.
Adams, D.C., Collyer, M.L., Kaliontzopoulou, A., Baken, E., 2021. Geomorph: software for geometric morphometric analyses. R package version 3.3.2. ⟨https://cran.r-project.org/package=geomorph⟩.
Alberch, P., 1981. Convergence and parallelism in foot morphology in the neotropical salamander genus *Bolitoglossa*. I. Function. Evolution 35, 84–100.
AmphibiaWeb. 2021. University of California, Berkeley, CA, USA. ⟨https://amphibiaweb.org⟩, (Accessed 8 September 2021).
Arnold, S.J., 1983. Morphology, performance and fitness. Am. Zool. 23, 347–361.
Baken, E.K., Adams, D.C., 2019. Macroevolution of arboreality in salamanders. Ecol. Evol. 9, 7005–7016.
Bardua, C., Fabre, A.C., Clavel, J., Bon, M., Das, K., Stanley, E.L., Blackburn, D.C., Goswami, A., 2021. Size, microhabitat, and loss of larval feeding drive cranial diversification in frogs. Nat. Commun. 12, 2403.
Blankers, T., Adams, D.C., Wiens, J.J., 2012. Ecological radiation with limited morphological diversification in salamanders. J. Evol. Biol. 25, 634–646.
Blomberg, S.P., Garland, T., Ives, A.R., 2003. Testing for phylogenetic signal in comparative data: behavioral traits are more labile. Evolution 57, 717–745.
Bonett, R.M., Blair, A.L., 2017. Evidence for complex life cycle constraints on salamander body form diversification. Proc. Natl. Acad. Sci. USA 114, 9936–9941.
Bonett, R.M., Hess, A.J., Ledbetter, N.M., 2020. Facultative transitions have trouble committing, but stable life cycles predict salamander genome size evolution. Evol. Biol. 47, 111–122.
Bonett, R.M., Steffen, M.A., Lambert, S.M., Wiens, J.J., Chippindale, P.T., 2014. Evolution of paedomorphosis in plethodontid salamanders: ecological correlates and re-evolution of metamorphosis. Evolution 68, 466–482.
Bonett, R.M., Ledbetter, N.M., Hess, A.J., Herrboldt, M.A., Denoël, M., 2021. Repeated ecological and life cycle transitions make salamanders an ideal model for evolution and development. Dev. Dyn. 251, 957–972.
Bookstein, F.L., 1997. Landmark methods for forms without landmarks: morphometrics of group differences in outline shape. Med. Image Anal. 1, 225–243.
Brandon, R.A., 1971. Correlation of seasonal abundance with feeding and reproductive activity in the Grotto Salamander (*Typhlotriton spelaeus*). Am. Midl. Nat. 86, 93–100.
Catalano, S.A., Goloboff, P., Giannini, N., 2010. Phylogenetic morphometrics (I): the use of landmark data in a phylogenetic framework. Cladistics 26, 539–549.
Darda, D.M., Wake, D.B., 2015. Osteological variation among extreme morphological forms in the Mexican salamander genus *Chiropterotriton* (Amphibia: Plethodontidae): morphological evolution and homoplasy. PLoS One 10 (6), e0127248.
Diefenbacher, E.H., 2008. Comparing Digit Morphology of an Arboreal Salamander with Potential Competitors (Ph.D. Thesis), pp. 59.
Dodd Jr., C.K., 1990. Postures associated with immobile woodland salamanders, genus *Plethodon*. Fla. Sci. 53, 43–49.
Duellman, W.E., Trueb, L., 1994. Biology of Amphibians. McGraw-Hill, New York.
Ebenman, B., 1992. Evolution in organisms that change their niches during the life cycle. Am. Nat. 139, 990–1021.
Edgington, H.A., Taylor, D.R., 2019. Ecological contributions to body shape evolution in salamanders of the genus *Eurycea* (Plethodontidae). PLoS One 14 (5), e0216754.
Estes, R., 1965. Fossil salamanders and salamander origins. Am. Zool. 5, 319–334.
Evelyn, C.J., Sweet, S.S., 2018. Southern Torrent Salamander (*Rhyacotriton variegatus*). Draft Species Account and Evaluation Form for Pacific Southwest Region Management Plan. Kueger, P. (coordinator). Regional Threatened and Endangered Species. USDA Forest Service, Pacific Southwest region.
Fabre, A.C., Bardua, C., Bon, M., Clavel, J., Felice, R.N., Streicher, J.W., Bonnel, J., Stanley, E.L., Blackburn, D.C., Goswami, A., 2020. Metamorphosis shapes cranial diversity and rate of evolution in salamanders. Nat. Ecol. Evol. 4, 1129–1140.
Franssen, R.A., Marks, S., Wake, D., Shubin, N., 2005. Limb chondrogenesis of the seepage salamander, *Desmognathus aeneus* (Amphibia: Plethodontidae). J. Morphol. 265, 87–101.
Freeman, S.L., Bruce, R.C., 2001. Larval period and metamorphosis of the Three-Lined Salamander, *Eurycea guttolineata* (Amphibia: Plethodontidae), in the Chattoga River Watershed. Am. Midl. Nat. 145, 194–200.
Fröbisch, N.B., Shubin, N.H., 2011. Salamander limb development: integrating genes, morphology, and fossils. Dev. Dyn. 240, 1087–1099.
Frost, D.R., 2021. Amphibian Species of the World: An Online Reference. Version 6.1 (Date of access). American Museum of Natural History, New York, USA. Electronic Database accessible at ⟨https://amphibiansoftheworld.amnh.org/index.php⟩.
Gao, K.Q., Shubin, N.H., 2012. Late Jurassic salamandroid from western Liaoning, China. Proc. Nat. Acad. Sci. USA 109, 5767–5772.
Goloboff, P., Catalano, S.A., 2011. Phylogenetic morphometrics (II). Cladistics 27, 42–51.
Goloboff, P., Farris, J., Nixon, K.T.N.T., 2003. TNT: Tree Analysis Using New Technology. Program and documentation. Available from the authors.
Goloboff, P.A., Catalano, S.A., 2016. TNT version 1.5, including a full implementation of phylogenetic morphometrics. Cladistics 32 (3), 221–238.
Goloboff, P.A., Farris, J.S., Nixon, K.C., 2008. TNT, a free program for phylogenetic analysis. Cladistics 24 (5), 774–786.
Gould, S.J., 2002. The Structure of Evolutionary Theory. Harvard University Press, Cambridge.
Grafen, A., 1989. The phylogenetic regression. Philos. Trans. R. Soc. Lond. B Biol. Sci. 326 (1233), 119–157.
Gray, J., 1968. Animal Locomotion. W. W. Norton & Company, New York.
Green, D.M., Alberch, P., 1981. Interdigital webbing and skin morphology in the neotropical salamander genus *Bolitoglossa*. J. Morphol. 170, 273–282.
Gűizado-Rodriguez, García-Vázquez, 2010. Thermal ecology of *Pseudoeurycea leprosa* (Caudata: Plethodontidae) from Sierra Ajusco. Herpetol. Bull. 111, 15–18.
Guns, P., Mitteroecker, P., Bookstein, F.L., 2005. Semilandmarks in three dimensions. In: Slice, D.E. (Ed.), Modern Morphometrics in Physical Anthropology. Springer, Boston, MA, pp. 73–98.
Hanken, J., 1982. Appendicular skeletal morphology in minute salamanders, genus *Thorius* (Amphibia: Plethodontidae): growth regulation, adult size determination, and natural variation. J. Morphol. 174, 57–77.
Hanken, J., 1984. Miniaturization and its effects on cranial morphology in plethodontids salamanders, genus *Thorius* (Amphibia: Plethodontidae). O. Osteological variation. Biol. J. Linn. Soc. 23, 55–75.
Hanken, J., 1992. Life-history and morphological evolution. J. Evol. Biol. 5, 549–557.
Hanken, J., Wake, D.B., 1994. Five new species of minute salamanders, genus *Thorius* (Caudata: Plethodontidae), from Northern Oaxaca, Mexico. Copeia 1994, 573–590.
Irschick, D.J., 2002. Evolutionary approaches for studying functional morphology: examples from studies of performance capacity. Integr. Comp. Biol. 42, 278–290.
Irschick, D.J., Losos, J.B., 1998. A comparative analysis of the ecological significance of maximal locomotor performance in Caribbean *Anolis* lizards. Evolution 52, 219–226.
Irschick, D.J., Jayne, B.C., 1998. Effects of incline on speed, acceleration, body posture and hindlimb kinematics in two species of lizard *Callisaurus draconoides* and *Uma scoparia*. J. Exp. Biol. 201, 273–287.
Jaekel, M., Wake, D.B., 2007. Developmental processes underlying the evolution of a derived foot morphology in salamanders. Proc. Natl. Acad. Sci. USA 104, 20437–20442.

Jetz, W., Pyron, R.A., 2018. The interplay of past diversification and evolutionary isolation with present imperilment across the amphibian tree of life. Nat. Ecol. Evol. 2, 850–858.
Jia, J., Gao, K.Q., 2016. A new hynobiid-like salamander (Amphibia, Urodela) from inner Mongolia, China, provides a rare case study of developmental features in an early Cretaceus fossil urodele. PeerJ. https://doi.org/10.7717/peerj.2499.
Jockusch, E.L., 1997. Geographic variation and phenotypic plasticity of number of trunk vertebrae in slender salamanders, *Batrachoseps* (Caudata: Plethodontidae). Evolution 51, 1966–1982.
Larson, A., Wake, D.B., Maxson, L.R., Highton, R., 1981. A molecular phylogenetic perspective on the origins of morphological novelties in the salamanders of the tribe Plethodontini (Amphibia, Plethodontidae). Evolution 35, 405–422.
Ledbetter, N.M., Bonett, R.M., 2019. Terrestriality constraints salamander limb diversification: implications for the evolution of pentadactyly. J. Evol. Biol. 32, 642–652.
Liedtke, H.C., Gower, D.J., Wilkinson, M., Gomez-Mestre, I., 2018. Macroevolutionary shift in the size of amphibian genomes and the role of life history and climate. Nat. Ecol. Evol. 2 (11), 1792–1799.
Losos, J.B., 2011. Seeing the forest for the trees: the limitations of phylogenies in comparative biology. Am. Nat. 177, 709–727.
Maiolino, S., Boyer, D.M., Rosenberger, A., 2011. Morphological correlates of the grooming claw in distal phalanges of platyrrhines and other primates: a preliminary study. Anat. Rec. 294, 1975–1990.
Michaud, M., Veron, G., Peigne, S., Blin, A., Fabre, A.C., 2018. Are phenotypic disparity and rate of morphologicalevolution correlated with ecological diversity in Carnivora? Biol. J. Linn. Soc. 124, 294–307.
Moran, N.A., 1994. Adaptation constraint in the complex life cycles of animals. Annu. Rev. Ecol. Syst. 25, 573–600.
Myers, P., R. Espinosa, C.S. Parr, T. Jones, G.S. Hammond, and T.A. Dewey, 2022. The Animal Diversity Web (online). Accessed at ⟨https://animaldiversity.org⟩.
O' Reilly, J.C., Summers, A.P., Ritter, D.A., 2000. The evolution of the functional role of trunk muscles during locomotion in adult amphibians. Am. Zool. 40, 23–135.
Olsen, A.M., Westneat, M.W., 2015. StereoMorph: an R package for the collection of 3D landmarks and curves using a stereo camera set-up. Methods Ecol. Evol. 6, 351–356.
Papenfuss, T.J., Wake, D.B., 1987. Two new species of plethodontid salamanders (genus Nototriton) from Mexico. Acta Zool. Mex. Nueva Ser. 21, 1–16.
Paradis, E., Schliep, K., 2019. ape 5.0: an environment for modern phylogenetics and evolutionary analyses in R. Bioinformatics 35, 526–528.
Parra-Olea, G., García-París, M., Wake, D.B., 2004. Molecular diversification of salamanders of the tropical American genus *Bolitoglossa* (Caudata: Plethodontidae) and its evolutionary and biogeographical implications. Biol. J. Linn. Soc. 81, 325–346.
R Core Team, 2020. R: A Language and Environment for Statistical Computing. R Foundation for Statistical Computing, Vienna, Austria. ⟨https://www.R-project.org/⟩.
Richarson, M.K., Gobes, S.M.H., Van Leeuwen, A.C., Polman, J.A.E., Pieau, C., Sánchez-Villagra, M., 2009. Heterochrony in limb evolution: developmental mechanisms and natural selection. J. Exp. Zool. (Mol. Dev. Evol.) 312 (B), 639–664.
Rodríguez Reyes, F.R., 2009. Dinámica poblacional del ajolote *Ambystoma altamirani* (Thesis). Univ. Nac. Autónoma de México, p. 80.
Rohlf, F., Slice, D., 1990. Extensions of the procrustes method for the optimal superimposition of landmarks. Syst. Zool. 39, 40–59.
Rong, Y.F., Vasilyan, D., Dong, L.P., Wang, Y., 2021. Revision of *Chunerpeton tianyiense* (Lissamphibia, Caudata): is it a cryptobranchid salamander? Palaeoworld. https://doi.org/10.1016/j.palwor.2020.12.001.
Rovito, S.M., Vásquez-Almazán, C.R., Papenfuss, T.J., 2010. A new species of *Bolitoglossa* (Caidata: Plethodontidae) from the Sierra de las Minas. Guatem. J. Herpetol. 44, 516–525.
Russell, A.P., Bauer, A., 1989. The morphology of the digits of the golden gecko *Calodactylodes aureus* and its implication for the occupation of rupicolous habitats. Amphib.-Reptil. 10, 125–140.
Shaffer, H.B., 1984. Evolution in a paedomorphic lineage. II. Allometry and form in the mexican ambystomatid salamanders. Evolution 38, 1207–1218.
Sherratt, E., Vidal-García, M., Anstis, M., Keogh, J.S., 2017. Adult frogs and tadpoles have different macroevolutionary patterns across the Australian continent. Nat. Ecol. Evol. 1, 1385–1391.
Tulli, M.J., Cruz, F.B., Herrel, A., Vanhooydonck, B., Abdala, V., 2009. The interplay between claw morphology and microhabitat use in neotropical iguanian lizards. Zoology 112, 379–392.
Uribe-Peña, Z. Ramírez-Bautista, R., Cuadernos, G.C.A., 2000. Anfibios y reptiles de las Serranías del Distrito Federal, México. Instituto de Biología, UNAM. México City, México.
Vitt, L.J., Caldwel, J.P., 2009. Herpetology: An Introductory Biology of Amphibians and Reptiles. Academic Press, San Diego.
Vučić, T., Sibinović, M., Vukov, T.D., Kolarov, N.T., Cvijanović, M., Ivanović, A., 2019. Testing the evolutionary constraints of metamorphosis: the ontogeny of head shape in *Triturus* newts. Evolution 73, 1253–1264.
Wainwright, P.C., Reilly, S.M., 1994. Ecological Morphology: Integrative Organismal Biology. University of Chicago Press, Chicago.
Wake, D.B., 1963. Comparative osteology of the plethodontid salamander genus *Aneides*. J. Morphol. 113, 77–118.
Wake, D.B., 1966. Comparative osteology and evolution of the lungless salamanders, Family Plethodontidae. Mem. South. Calif. Acad. Sci. 4, 1–111.
Wake, D.B., 1987. Adaptive radiation of salamanders in Middle American cloud forests. Ann. Mo. Bot. Gard. 74, 242–264.
Wake, D.B., 2009. What salamanders taught us about evolution. Annu. Rev. Ecol. Evol. Syst. 40, 333–352.
Wake, D.B., Brame Jr., A.H., 1966. Notes on South American salamanders of the genus *Bolitoglossa*. Copeia 1966, 360–363.
Wake, D.B., Lynch, J.F., 1976. The distribution, ecology and evolutionary history of plethodontid salamanders in tropical America. Nat. Hist. Mus. Los Angel Co. Sci. Bull. 25, 1–65.
Wake, D.B., Roth, G., 1989. Complex Organismal Functions: Integration and Evolution in Vertebrates. John Wiley & Sons, Chichester.
Wake, D.B., Hanken, J., 1996. Direct development in the lungless salamanders: what are the consequences for developmental biology, evolution and phylogenesis? Int. J. Dev. Biol. 40, 859–869.
Wake, D.B., Shubin, N., 1998. Limb development in the Pacific Giant salamanders, *Dicamptodon* (Amphibia, Caudata, Dicamptodontidae). Can. J. Zool. 76, 2058–2066.
Wake, D.B., Campbell, J.A., 2001. An aquatic plethodontid salamander from Oaxaca, Mexico. Herpetologica 57, 509–514.
Wang, Y., Gao, K., 2008. Amphibians. In: Chang, M. (Ed.), The Jehol Fossils. Academic press, New York, pp. 76–85.
Wiens, J.J., Hoverman, J.T., 2008. Digit reduction, body size, and paedomorphosis in salamanders. Evol. Dev. 10, 449–463.
Wollenberg Valero, K.C., Garcia-Porta, J., Rodríguez, A., Arias, M., Shah, A., Randrianiaina, R.D., Brown, J.L., Glaw, F., Amat, F., Künzel, S., Metzler, D., Isokpehi, R.D., Vences, M., 2017. Transcriptomic and macroevolutionary evidence for phenotypic uncoupling between frog life history phases. Nat. Commun. 8, 15213.